Specification of Spacecraft Flexible Appendage Rigidity

S.M. Seltzer*
Control Dynamics Co., Huntsville, Ala.
and
H.L. Shelton†
NASA George C. Marshall Space Flight Center, Ala.

A method for specifying the required degree of rigidity of spacecraft flexible appendages is needed. Present engineering practice usually is to set a lower limit below which bending mode frequencies may not lie. Usually no constraint is established for the other modal characteristics (modal gain or deflection and modal damping ratio). In this paper, an analytical technique is set forth which allows the control systems engineer to establish values for the frequency, damping ratio, and modal gain (deflection) of the first several bending modes. The technique is applied to specifying solar panel rigidity constraints for the NASA Space Telescope.

Nomenclature

A = modulus of $G(s)$
C.E.(s) = characteristic equation
$G(s)$ = $\Phi_A(s)/\Phi_\epsilon(s)$
$G_C(s)$ = transfer function representing the controller
$G_{FB}(s)$ = transfer function representing flexible appendage dynamics
$G_{RB}(s)$ = transfer function representing rigid body dynamics
I = overall vehicle moment of inertia
K_{Bj} = modal gain of the jth normal mode
K_D = derivative of position feedback gain
K_I = integral of position feedback gain
K_P = position feedback gain
M = order of C.E. (s)
N = total number of normal modes selected to describe the system
T_C = torque command
X_k = real part of s^k
Y_k = imaginary part of s^k
a_{Bj} = $K_{Bj}I$
a_D = K_D/I
a_I = K_I/I
a_k = coefficients of s^k in open-loop transfer function
a_P = K_P/I
$b_k, c_k, d_k, e_k, f_k, h_k$ = coefficients of terms in a_k
f_{Bj} = $\omega_{Bj}/2\pi$
f_k = kth coefficient of C.E. (s)
i = imaginary $(\sqrt{-1})$
j = subscript referring to a particular mode
k = index associated with numerator of closed-loop transfer function
n_k = kth coefficient of numerator of closed-loop transfer function
s = Laplace operator
W = imaginary part of $G(s)$
ℓ = index
Σ = real part of $G(s)$
$\alpha_k, \beta_k, \gamma_k, \delta_k$ = coefficient of terms in f_k
ζ = system damping ratio
ζ_{Bj} = damping ratio of the jth normal mode
θ = argument of $G(s)$
σ = real root of system
ϕ_A = actual vehicle attitude
ϕ_C = commanded vehicle attitude
ϕ_ϵ = position attitude error
ω_{Bj} = natural frequency of the jth normal mode
ω_n = system natural frequency

Presented as Paper 77-1098 at the AIAA Guidance and Control Conference, Hollywood, Florida, Aug. 8-10, 1977; submitted Sept. 19, 1977; revision received April 7, 1978.

Index categories: Analytical and Numerical Methods; Spacecraft Dynamics and Control.

*Consultant. Associate Fellow AIAA.
†Leader, Stabilization and Control Team, Pointing Control Systems Branch, Systems Dynamics Laboratory.

I. Introduction

DURING the preliminary design phases of a spacecraft, the required degree of rigidity of flexible appendages usually is stated first by the control system engineer. This is after consultation with the structural dynamics engineer, who in turn must have inputs from the materials engineer. This first design constraint usually is stated in terms of a lower limit beneath which the flexible appendages' bending modes must not lie. This limit is set by rule-of-thumb to preclude dynamic interaction between the spacecraft attitude control system and the flexible appendages. Usually it involves a separation of the control system frequency (bandwidth) and the lowest (or first) bending mode frequency identified with the flexible appendages. No constraint is established for the other modal characteristics, such as modal gain or deflection and modal damping.

A technique (and several variations thereof) is set forth in this paper which gives the control systems engineer an analytical tool for prescribing constraints upon the modal frequencies, modal damping, and modal gains. The technique involves use of the parameter plane design tool which is adapted by the authors to use in specifying appendage rigidity parameters.[1] As will be shown, the flexible appendage designer is given a tradeoff between numerical values he may choose for modal characteristics (parameters) rather than merely a single frequency above which the appendage bending frequencies must lie.

The first task at hand for the control systems engineer is to select a model of the spacecraft, its flexible appendages, and the attitude control system. Current aerospace practice traditionally describes vehicle flexibility in terms of overall vehicle normal modes.[2] This paper will follow suit in order to prescribe a design tool that will be useful for most practicing engineers. It is pointed out, however, that a more useful tool would cast the flexibility characteristics in terms of appendage coordinates rather than overall vehicle coordinates. This can be done by using the hybrid-coordinate method.[3] The only apparent disadvantage of this approach is that most aerospace

design organizations are set up to describe vehicle dynamics in terms of overall vehicle normal coordinates. In this paper, the spacecraft will be modeled as a rigid body with an attached flexible appendage represented in normal mode form.

II. Model

For analytical tractability the spacecraft model is simplified to portray the rotational dynamics in a single plane of motion. The flexible appendage is characterized dynamically by the first (lowest) bending mode of the overall vehicle which is associated primarily with the flexible appendage. A method for including the effects of more than this lowest mode is postulated, and a two-bending mode case is presented. The spacecraft attitude controller is assumed to be a standard position-integral-derivative (PID) state feedback controller. The model does not account for cross-coupling dynamics that may exist. The prescribed characteristics that result from application of the technique described herein would have to be evaluated dynamically on a computer simulation in accordance with standard engineering design practice. A block diagram of the model used is shown in Fig. 1, where vehicle dynamics are described by the rigid body transfer function,

$$G_{RB}(s) = (Is^2)^{-1} \tag{1a}$$

and the "primarily flexible body" transfer function,

$$G_{FB}(s) = \sum_{j=1}^{N} K_{B_j} / (s^2 + 2\zeta_{Bj}\omega_{Bj}s + \omega_{Bj}{}^2) \tag{1b}$$

where I is the principal moment of inertia of the total vehicle about an axis perpendicular to the plane in.which the vehicle is assumed to be rotating; j refers to each of the total of N normal modes that are selected to describe the flexible dynamics of the spacecraft appendages; K_{Bj} is the modal gain (comprised of the mode shape deflections and the generalized modal mass associated with the jth mode shape), ζ_{Bj} represents the damping ratio associated with the jth mode, and ω_{Bj} represents the natural frequency of the jth mode. The PID controller is represented by $G_C(s) = K_P + K_I/s + K_D s$, where K_P, K_I, and K_D are the gains associated with the position error, integral of position error, and derivative of position error states. The position attitude error (ϕ_ϵ) is the difference between the vehicle commanded attitude (ϕ_C) and the actual attitude (ϕ_A). The controller generates a torque command (T_C) which acts on the vehicle dynamics to produce the vehicle attitude (ϕ_A). It is assumed herein that the torque command is equal to the actual applied torque. When $N=1$ the closed-loop transfer function between $\phi_A(s)$ and $\phi_C(s)$ is found to be

$$\phi_A(s)/\phi_C(s) = \left(\sum_{k=0}^{4} n_k s^k\right) \Big/ \text{C.E.(s)} \tag{2}$$

where C.E.(s) represents the characteristic equation of the system,

$$\text{C.E.}(s) = \sum_{k=0}^{M} f_k s^k = 0 \tag{3}$$

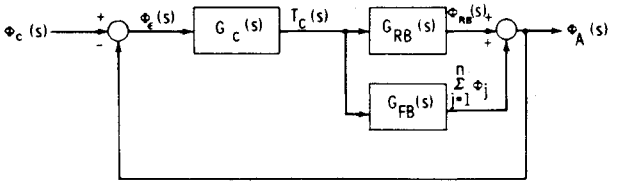

Fig. 1 Spacecraft model.

with $M=5$. The coefficients n_k and f_k are defined in Table 1, for $N=1$, where $a_P = K_P/I$, $A_I = K_I/I$, $a_D = K_D/I$, and $a_{BI} = K_{BI}I$.

III. Analysis Technique

The technique described herein is iterative in application. First, numerical values for the PID controller gains are selected, using pole placement or other appropriate techniques to obtain desired system responses. This ignores the dynamic effects of the flexible appendages at first. Then two of the three flexible body parameters (K_{BI}, ζ_{BI}, ω_{BI}) are selected (in a planar presentation, the dynamic effect of varying two parameters is shown easily). The region on this two-parameter plane in which a stable response exists (for the idealized linear, time-invarient system) is determined next. A factor of safety must be incorporated to take into account variations in the flexible body parameters that occur during the design and development phase. Three such factors of safety are associated with 1) requiring the system damping ratio (ζ) to be greater than a selected value (say $\zeta = 0.1$), 2) placing actual tolerances on the two selected bending parameters, and 3) establishing a combination gain-margin/phase-margin requirement. The region on the two-parameter plane that insures the selected factor of safety may then be filled with loci of constant ζ's (plotted as functions of the system natural frequency ω_n) and constant σ's (real root locations). Each curve of constant ζ corresponds to one pair of system complex conjugate roots, and each σ curve corresponds to one system real root. Now one can see the dynamic effect (in terms of system pole locations) of selecting a set of values of the two parameters for the particular PID gain values chosen. If unsatisfactory, one must review and alter one's initial choice of PID gain values. When only one bending mode is used to portray appendage flexibility, one sees from Eq. (3) that there exist five system roots. One must expect to find intersections of sufficient number of ζ contours (two roots each) and σ contours (one root each) at each point in the two-parameter plane to account for all five roots. Now the system dynamics may be determined, either qualitatively (from general knowledge of the effect of root locations) or quantitatively [using Eq. (2) and evaluating the residues associated with the selected roots]. If it is felt that the second bending mode will significantly affect the system response, the next iteration will consist of incorporating the second mode into the system characteristic equation, leading to a seventh-order equation. In a similar manner to the foregoing (using the already selected value for PID gains and now ζ_{BI}, ω_{BI}, and K_{BI}), a two-parameter plane is used to specify values for ζ_{B2}, ω_{B2}, and K_{B2}. This, then, is the general analytical approach prescribed. It now will be defined in more detail.

Table 1 Closed-loop transfer function coefficients for $N=1$

k	f_k	n_k
0	$a_I\omega_{BI}^2$	$a_I\omega_{BI}^2$
1	$2a_I\omega_{BI}\omega_{BI} + a_P\omega_{BI}^2$	$2a_D\omega_{BI}\zeta_{BI} + a_P\omega_{BI}^2$
2	$2a_P\omega_{BI}\zeta_{BI} + a_D\omega_{BI}^2 + a_Ia_{BI} + a_I$	$2a_P\omega_{BI}\zeta_{BI} + a_Ia_{BI} + a_D\omega_{BI}^2 + a_I$
3	$2a_D\omega_{BI}\zeta_{BI} + \omega_{BI}^2 + a_Pa_{BI} + a_P$	$2a_D\omega_{BI}\zeta_{BI} + a_{PBI} + a_p$
4	$2\omega_{BI}\zeta_{BI} + a_Da_{BI} + a_D$	$a_Da_{BI} + a_D$
5	1	0

Assume structural flexibility is described by the first bending mode and its associated parameters a_{Bl}, ζ_{Bl}, and ω_{Bl}. Equation (3) and Table 1 are applicable. One first selects the pair of parameters which he chooses to portray flexibility. Assume it is desired to select an a_{Bl} vs ζ_{Bl} plane (for various values of ω_{Bl}, chosen one at a time). Applying parameter plane techniques to Eq. (3) one first defines

$$s^k = X_k + iY_k \tag{4}$$

where

$$X_k = 2\zeta\omega_n X_{k-1} - \omega_n^2 X_{k-2} \tag{5a}$$

$$Y_k = 2\zeta\omega_n Y_{k-1} - \omega_n^2 Y_{k-2} \tag{5b}$$

and $X_0 = 1$, $Y_0 = 0$, $X_1 = \zeta\omega_n$, and $Y_1 = \omega_n (1-\zeta^2)^{1/2}$.
If one substitutes Eqs. (4 and 5) into Eq. (3) one can then separate the real and imaginary parts into two similtaneous equations:

$$A_\ell \omega_{Bl}^2 + B_\ell \omega_{Bl} + G_\ell a_{Bl} + D_\ell = 0, \ \ell = 1,2 \tag{6}$$

where

$$A_1 = \sum_{k=0}^{5} a_k X_k, A_2 = \sum_{k=0}^{5} a_k Y_k, B_1 = \sum_{k=0}^{5} \beta_k X_k, B_2 = \sum_{k=0}^{5} \beta_k Y_k,$$

$$D_1 = \sum_{k=0}^{5} \delta_k X_k, D_2 = \sum_{k=0}^{5} \delta_k Y_k, G_1 = \sum_{k=0}^{5} \gamma_k X_k, G_2 = \sum_{k=0}^{5} \gamma_k Y_k$$

The terms a_k, β_k, γ_k, and δ_k are found by writing f_k of Eq. (3) as

$$f_k = a_k \omega_{Bl}^2 + \beta_k \omega_{Bl} + \gamma_k a_{Bl} + \delta_k \tag{7}$$

One can solve Eq. (6) for ω_{Bl} and a_{Bl} as functions of the independent argument ω_n for selected values of ζ_{Bl}:

$$\omega_{Bl} = [-B_5 + (B_5^2 - 4A_1 B_5)^{1/2}]/2A_1 \tag{8a}$$

$$a_{Bl} = -(D_4 + B_4 \omega_{Bl})/G_4 \tag{8b}$$

where

$$B_5 = B_1 - G_1 B_4/G_4, \ D_5 = D_1 - G_1 D_4/G_4,$$

$$B_4 = A_2 B_1 - A_1 B_2, \ G_4 = A_2 G_1 - A_1 G_2, \ D_4 = A_2 D_1 - A_1 D_2$$

The system stability boundary is determined by setting $\zeta = 0$ in Eqs. (5) resulting stable regions are shown in Fig. 2. One also can let ζ take on values from 0 to 1 and plot ζ contours (as functions of ω_n). Using numerical values from Sec. IV, typical ζ contours are shown on Fig. 3. The σ contours are found by substituting $s = \sigma$ in Eq. (3) and rearranging the terms, leading to

$$\omega_{Bl} = -B_3 \pm [B_3^2 - 4A_3 (G_3 a_{Bl} + D_3)]^{1/2}/2A_3 \tag{9}$$

where A_3, B_3, D_3, and G_3 are defined as

$$A_3 = \sum_{k=0}^{5} a_k \sigma^k, \quad B_3 = \sum_{k=0}^{5} \beta_k \sigma^k,$$

$$D_3 = \sum_{k=0}^{5} \delta_k \sigma^k, \quad \text{and} \quad C_3 = \sum_{k=0}^{5} \gamma_k \sigma^k$$

Typical σ contours are shown on Fig. 4. Where appropriate, additional stability boundaries are found by setting $\sigma = 0$ and $\sigma \to \infty$ (these stability boundaries do not exist in the example presented herein).

Alternately, one can portray dynamic characteristics on the $\zeta_{Bl} - a_{Bl}$ or the $\zeta_{Bl} - \omega_{Bl}$ planes by writing f_k of Eq. (3) as a function of either ζ_{Bl}, a_{Bl}, or ζ_{Bl}, ω_{Bl} and repeating the procedure that has been outlined.

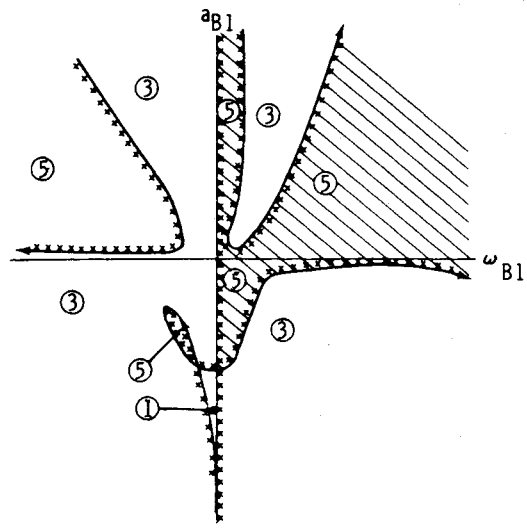

Fig. 2 Stable region (ω_{Bl}, a_{Bl} parameter plane).

This same parameter plane technique can be used to define allowable bending parameters for a given gain and phase margin. The open-loop transfer function can be set equal to the desired gain and phase margin, i.e.,

$$G(s) = \phi_A(s)/\phi_\epsilon(s) = A \angle \theta = \Sigma + iW \tag{10}$$

The right side of Eq. (10) can be used to define the boundary for the desired stability margin. Figure 5 shows the forbidden region in the $G(s)$ plane for a prescribed stability margin. Equation (10) can be written in the form

$$\sum_{k=0}^{5} a_k s^k = 0 \tag{11}$$

The coefficients a_k for the rigid body and one bending mode are defined in Table 2, written in the following form:

$$a_k = (b_k + ic_k) a_{Bl} + (d_k + ie_k) \zeta_{Bl} + (f_k + ih_k), \qquad (k = 0, 1, \ldots, n) \tag{12}$$

This technique also is iterative in nature. First, the PID controller gains are selected for the rigid body system. The criteria for this selection may be conventional in nature to provide a particular response (by pole placement or other techniques), a specific stability margin, or a particular controller bandwidth. Next, two of the three flexible body parameters (a_{Bl}, ζ_{Bl}, ω_{Bl}) are selected for a planar presentation, to show the effect of varying the two parameters on the system gain and phase margins. The stable region (i.e., $\Sigma = -1$, $W = 0$) for the two bending parameters must be determined. This is equivalent to setting $\zeta = 0$ in Eq. (5). Then, values for the two bending parameters are determined for the values of Σ and W corresponding to the boundaries describing the specified gain and phase margins. Since the Nyquist plot alone is not sufficient to determine stability, the bending parameter values corresponding to Σ and W values in the foregoing must lie in the stable region. Once all of the plots corresponding to the forbidden region boundaries (usually the corners) have been made, the most stringent plot or envelope of plots will be labeled as the requirement on the two chosen bending parameters. If a_{Bl} and ζ_{Bl} are the parameters chosen to define the gain margin requirement boundary in the

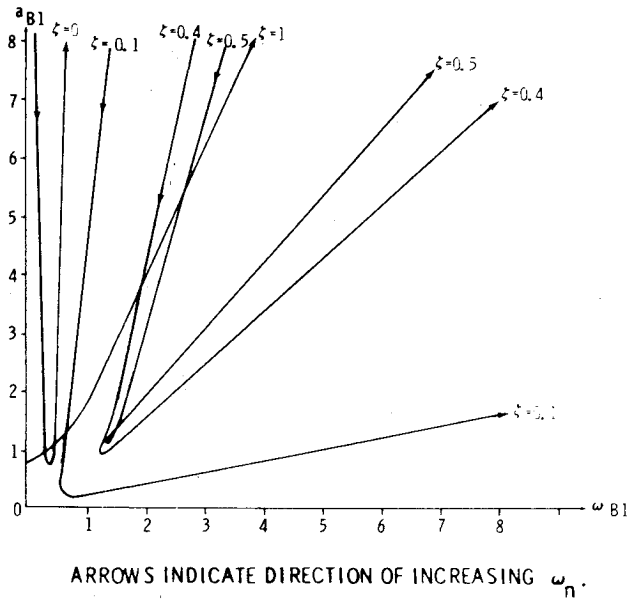

Fig. 3 ζ contours (ω_{Bl}, a_{Bl} parameter plane).

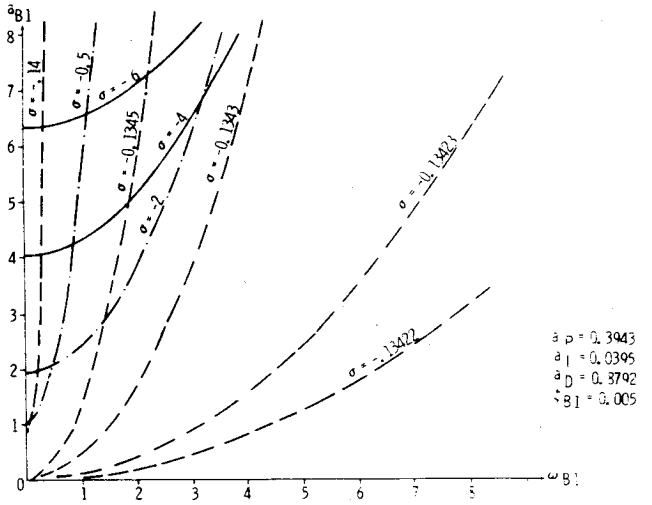

Fig. 4 σ contours (ω_{Bl}, a_{Bl} parameter plane).

parameter plane, the bending frequency ω_{Bl} would be an independent variable. The a_{Bl} vs ζ_{Bl} margin boundaries would then be computed vs bending frequency (ω_{Bl}). Then bending gain a_{Bl} can be read from the $a_{Bl}-\zeta_{Bl}$ parameter plane plots and plotted vs ω_{Bl}. Following the same approach shown earlier in this paper, a parameter plane plot of a a_{Bl} vs ω_{Bl} for a specified gain/phase margin can be developed. (This development will not be shown in this paper.)

The solution of the parameter plane equations for a specified gain/phase margin boundary will be shown. Assume it is desired to select an a_{Bl} vs ζ_{Bl} plane for various values of ω_{Bl}, chosen one at a time. Applying the parameter plane technique to Eq. (11) one must map the $s=i\omega$ boundary in the s plane (just as one normally does when applying the Nyquist criteria) into the parameter plane. This is done by substituting Eqs. (4) and (5) into Eq. (11); one then can separate the real and imaginary parts into two simultaneous equations:

$$\tilde{B}_\ell a_{Bl}+\tilde{G}_\ell \zeta_{Bl}+\tilde{D}_\ell=0, \quad \ell=1,2 \tag{13}$$

where

$$\tilde{B}_1=\sum_{k=0}^{5}(b_kX_k-c_kY_k), \quad \tilde{B}_2=\sum_{k=0}^{5}(b_kY_k+c_kX_k),$$

$$\tilde{G}_1=\sum_{k=0}^{5}(d_kX_k-e_kY_k), \quad \tilde{G}_2=\sum_{k=0}^{5}(d_kY_k+e_kX_k),$$

$$\tilde{D}_1=\sum_{k=0}^{5}(f_kX_k-h_kY_k) \quad \tilde{D}_2=\sum_{k=0}^{5}(f_kY_k+h_kX_k)$$

The b_k, c_k, d_k, e_k, f_k, h_k's are defined by Eq. (12). One can now solve Eq. (13) for a_{Bl} and ζ_{Bl} as functions of the independent variable ω_n for selected values of ω_{Bl}:

$$a_{Bl}=(\tilde{G}_1\tilde{D}_2-\tilde{G}_2\tilde{D}_1)/\Delta \tag{14a}$$

$$\zeta_{Bl}=(\tilde{B}_2\tilde{D}_1-\tilde{B}_1\tilde{D}_2)/\Delta \tag{14b}$$

where

$$\Delta=\tilde{B}_1\tilde{G}_2-\tilde{B}_2\tilde{G}_1 \tag{14c}$$

As stated previously, the stability boundary must be found first. Once the stability boundary is determined in the a_{Bl} vs

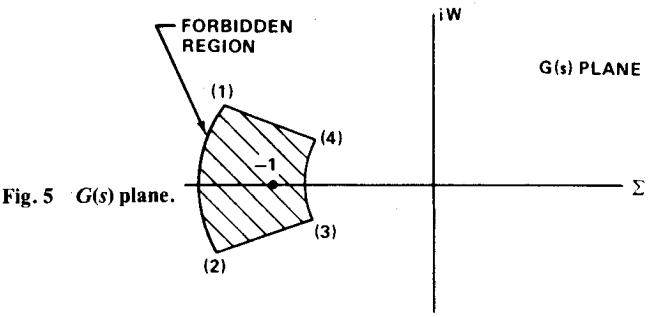

Fig. 5 $G(s)$ plane.

Table 2 Open-loop transfer function coefficient for rigid body and one bending mode

k	$(b+ic)$	$(d+ie)$	$(f+ih)$
0	0	0	$a_I\omega_{Bl}^2$
1	0	$2a_I\omega_{Bl}\zeta_{Bl}$	$a_P\omega_{Bl}^2$
2	a_Ia_{Bl}	$2a_p\omega_{Bl}\zeta_{Bl}$	$a_I+a_D\omega_{Bl}^2$
3	a_Pa_{Bl}	$2a_D\omega_{Bl}\zeta_{Bl}$	$(a_p+\Sigma\omega_{Bl}^2)+iW\omega_{Bl}^2$
4	a_Da_{Bl}	$[(2\omega_{Bl}\Sigma+i(2\omega_{Bl}W)]\zeta_{Bl}$	a_D
5	0	0	$\Sigma+iW$

ζ_{Bl} parameter plane, the specified margin boundaries are determined by setting Σ and W to the proper values to define the forbidden region of the $G(s)$ plane. Only the $a_{Bl}-\zeta_{Bl}$ curves in the stability region are considered beyond this point. The most stringent plot or envelope of plots in the stable region of the $a_{Bl}-\zeta_{Bl}$ parameter plane defines the allowable gain and damping to provide the specified system gain and phase margin. This process can be repeated for the entire expected range of ω_{Bl}. The same approach shown earlier can be applied to construct the $\omega_{Bl}-a_{Bl}$ parameter plane.

Often the required portion of the $a_{Bl}-\zeta_{Bl}$ will contain values of ζ_{Bl} that are impractical from a structural point of view. When this is the case, one should quote as a requirement only those segments of the curve corresponding to reasonable (as defined by the structural dynamics engineer) values of ζ_{Bl}.

Once the allowable a_{Bl} has been determined for the single bending mode, the same approach can be applied to the second bending mode. The values for a_{Bl}, ζ_{Bl}, and ω_{Bl} from the single bending mode will be fixed just as are the control gains and the rigid body inertia. The parameter plane equations can be written and solved for the allowable second

Table 3 Open-loop transfer function coefficient for rigid body and two bending modes

k	$(b+ic)$	$(d+ie)$
0	0	0
1	0	$[2a_I\omega_{B2}\omega_{BI}^2]$
2	$[a_I\omega_{BI}^2]$	$[2a_P\omega_{B2}\omega_{BI}^2+4a_I\zeta_{BI}\omega_{BI}\omega_{B2}]$
3	$[a_P\omega_{BI}^2+2a_I\zeta_{BI}\omega_{BI}^2)$	$[2a_D\omega_{B2}\omega_{BI}^2+2a_I(\omega_{B2}+a_{BI}\omega_{B2})+4a_P\zeta_{BI}\omega_{BI}\omega_{B2}]$
4	$[a_D\omega_{BI}^2+2a_P\zeta_{BI}\omega_{BI}+a_I)$	$[2\omega_{B2}\omega_{BI}^2\Sigma+2a_P(\omega_{B2}+a_{BI}\omega_{B2})+4a_D\zeta_{BI}\omega_{BI}\omega_{B2}]+i[2\omega_{B2}\omega_{BI}^2W]$
5	$[a_P+2a_D\zeta_{BI}\omega_{BI})$	$[2a_D(\omega_{B2}+a_{BI}\omega_{BI})+\Sigma\omega_{B2}\zeta_{BI}\omega_{BI}]+i[4W\omega_{B2}\zeta_{BI}\omega_{BI}]$
6	$[a_D]$	$[2\Sigma\omega_{B2}]+i[2W\omega_{B2}]$
7	0	0

k	$(f+ih)$
0	$[a_I\omega_{B2}^2\omega_{BI}^2]$
1	$[a_P\omega_{B2}^2\omega_{BI}^2+2a_I\zeta_I\omega_I\omega_2^2]$
2	$[a_I(\omega_{BI}^2+\omega_{B2}^2+a_{BI}\omega_{B2}^2)+a_D\omega_{B2}^2\omega_I^2+2a_P\zeta_{BI}\omega_{BI}\omega_{B2}^2]$
3	$[a_P(\omega_{BI}^2+\omega_{B2}^2+a_{BI}\omega_{B2}^2+2a_D\zeta_{BI}\omega_{BI}\omega_{B2}^2)+\Sigma\omega_{B2}^2\omega_{BI}^2+2a_I\zeta_{BI}\omega_{BI}]+i[W\omega_{B2}^2\omega_{BI}^2]$
4	$[a_D(\omega_{BI}^2+\omega_{B2}^2+a_{BI}\omega_{B2}^2)+2\Sigma\zeta_{BI}\omega_{BI}\omega_{B2}^2+2a_P\zeta_{BI}\omega_{BI}+a_I(1+a_{BI}))]+i[2W\omega_{B2}^2\zeta_{BI}\omega_{BI}]$
5	$[\Sigma(\omega_{BI}^2+\omega_{B2}^2)+2a_P(1+a_{BI})+2a_D\zeta_{BI}\omega_{BI}]+i[W(\omega_{BI}^2+\omega_{B2}^2)]$
6	$[a_D(1+a_{BI})+2\Sigma\zeta_{BI}\omega_{BI}]+i[2W\zeta_{BI}\omega_{BI}]$
7	$[\Sigma+iW]$

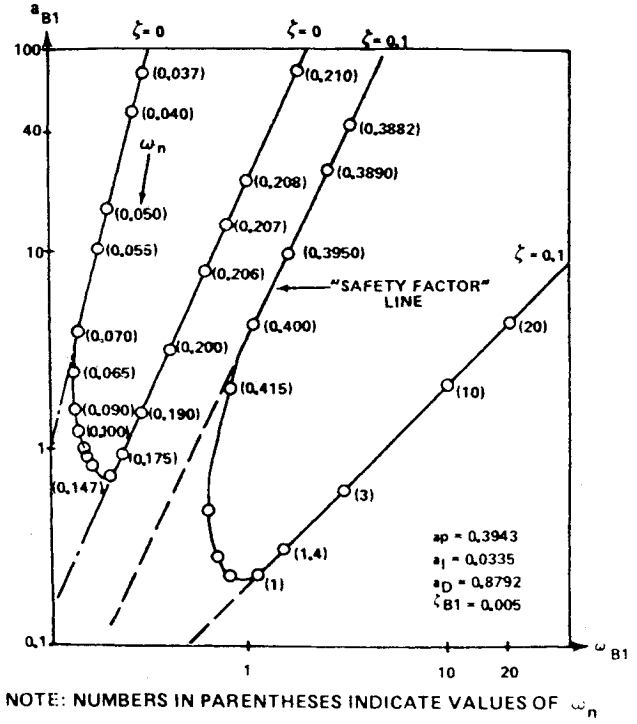

Fig. 6 Constraint prescription on ω_{BI}, a_{BI} plane.

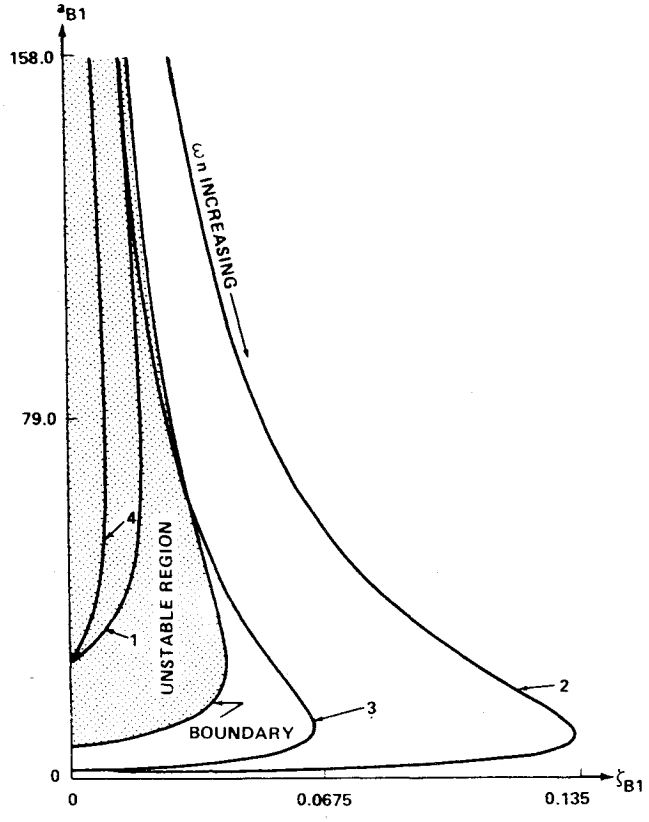

Fig. 7 a_{BI} vs ζ_{BI} parameter plane.

bending mode gain (a_{B2}) vs the second bending mode damping (ζ_{B2}). The coefficients of Eq. (11) for the two bending mode cases are shown in Table 3. If structural flexibility is to be described by two (rather than one) bending modes, the additional degrees of freedom introduced may be described by the modal gain, modal frequency, and modal damping (a_{B2}, ω_{B2}, ζ_{B2}) associated with the additional structural mode. In this case $N=2$ in Eq. (1), and $M=7$ in Eq. (3). Solving the parameter plane equations for a specified stability margin as before, one can generate the $a_{B2}-\zeta_{B2}$ parameter plane contours.

IV. Example

The foregoing technique will be applied to specify the NASA Space Telescope (ST) solar panel rigidity constraints.[4]

Assume that the principal moment of inertia about the telescope line of sight (ST *VI* axis) is $I=23{,}185$ kg·m^2 (updated value from that shown in Ref. 4.) Acceptable rigid body characteristics for the dynamics about the *VI* axis accrue if numerical values for control gains are selected as $K_P=9{,}143$ N·m/rad, $K_I=915$ N·m/s, and $K_D=20{,}383$ N·m·s/rad^2, yielding $a_P=0.3943$ (rad s^2)$^{-1}$, $a_I=0.0395$ (rad s^3)$^{-1}$, and $a_D=0.8792$ (rad^2/s)$^{-1}$, respectively. The corresponding rigid body system would have a natural frequency (ω_n) of 6.0 rad/s and a damping ratio (ζ) of 0.7.

If $\omega_{BI}-a_{BI}$ parameter plane is selected for this numerical example, the $\zeta=0$ and $\zeta=0.1$ contours may be mapped using

Table 4 Forbidden region corner definitions

Corner no.	$\Sigma + iW$
1	$-1.30 + i0.75$
2	$-1.30 - i0.75$
3	$-0.65 - i0.375$
4	$-0.75 + i0.375$

Eqs. (8). These are shown on Fig. 6. The other ζ contours and the σ contours resulting from use of Eq. (9) have been omitted for clarity. This time the second mentioned factor of safety, i.e., placing actual tolerances on the two selected bending parameters ω_{Bl} and a_{Bl}, is applied. A value of $\zeta_{Bl} = 0.005$ is used for this example. In this case, a "safety factor" line may be drawn parallel to the right-hand portion of the $\zeta = 0$ stability boundary. Suppose that one wishes to guard against ω_{Bl} changing its predicted value by a factor of 2 (or less) without causing system instability. The "safety factor" line would then lie approximately on the left-hand asymptote of the $\zeta = 0.1$ contour. Observe that, if ω_{Bl} does not change its value from the predicted one, then a_{Bl} can change its predicted value by a factor of approximately 3⅓ without causing system instability. In practice both ω_{Bl} and a_{Bl} values probably will change. As long as the combined effect of these changes remains within the bounds just stated, system stability will not be endangered. The same argument applies to predicted values for ζ_{Bl}. The curves on the $\omega_{Bl} - a_{Bl}$ plane can then be repeated for other values of ζ_{Bl} and a three-dimensional (ω_{Bl}, a_{Bl}, ζ_{Bl}) "safety factor" constraint surface can be developed. The system response to a selected input now can be calculated readily by using Eq. (2) and the residues associated with the chosen root locations. In similar manner, $\zeta_{Bl} - a_{Bl}$ or $\omega_{Bl} - \zeta_{Bl}$ parameter planes may be selected. These have been omitted for the sake of brevity.

The third factor of safety approach (asociated with gain and phase margins) is applied next. It will be applied to the case of one bending mode, using the $a_{Bl} - \zeta_{Bl}$ parameter plane shown in Fig. 7. For this example, only positive values of a_{Bl} and ζ_{Bl} are considered. Observing the plot one notices that the stable region is identified. The allowable $a_{Bl} - \zeta_{Bl}$ curves for the four corners of the forbidden region are shown. For this example, the Σ's and W's defining the forbidden region are defined in Table 4. To use the information in Fig. 7, one must consider only the curves in the stable region of the parameter plane. The entire curve for corner 2 and approximately one half of the curve for corner 3 are in the stable region. To determine the most stringent curve relative to guaranteeing the specified stability margins, one can apply the shading rule[1] to the curve for each boundary corner just as it is applied to determine the stable region. Following this shading rule, one can determine that any point on the corner 2 curve is stable and will not violate the other corner constraints; therefore, the corner 2 curve is considered the most stringent. The corner 2 curve would in this example be quoted as the $a_{Bl} - \zeta_{Bl}$ requirement curve for a fixed ω_{Bl}. For this curve, ω_{Bl} is 0.628 rad/s.

To verify that the approach was successful, values of a_{Bl} and ζ_{Bl} were read from Fig. 7 and used in the generation of an open-loop Nyquist open at the actuator. In looking at the system Nyquist plot one can observe that the specified stability margin has been met. Using the same technique and varying the ω_{Bl} over the expected range, one can then determine the allowable a_{Bl} vs f_{Bl} ($\omega_{Bl} = 2\pi f_{Bl}$). For this example, such a plot is a straight line (on log-log paper) over the range of interest for the stability margin specified by the boundary defined in Table 4 with $\zeta_{Bl} = 0.005$. As mentioned previously, this allowable bending gain (a_{Bl}) vs bending frequency (ω_{Bl}) is felt to be the most useful to the structural dynamicist and structural designer.

V. Conclusions

A means of analytically describing the required degree of rigidity for a spacecraft's flexible appendages is set forth. This is done by establishing constraints in terms of vehicle modal characteristics, herein defined as modal frequency (ω_{Bj}), modal damping (ζ_{Bj}), and modal gain (K_{Bj}). The shortcomings of the technique are the usual shortcomings associated with analytical methods – the limitations associated with the order of the equations that can be handled practically. However, an iterative method is prescribed for handling a system whose structural flexibility is described by more than one normal mode. The current practice is to specify appendage rigidity only in terms of modal frequency. This practice usually is implemented by stating that all modal frequencies must be above a particular frequency which is usually established as being some multiple of the control frequency (or bandwidth). The advantage of the technique set forth in this paper over existing methods is that structural rigidity is specified in terms of several rather than one modal characteristics, giving the appendage designer more freedom.

References

[1] Siljak, D.D., *Nonlinear Systems,* John Wiley and Sons, New York, 1969, pp. 1-106.

[2] Hurty, W.C. and Rubinstein, M.F., *Dynamics of Structures,* Prentice-Hall, Englewood Cliffs, N.J., 1964, pp. 110-140.

[3] Likins, P.W., *Dynamics and Control of Flexible Space Vehicles,* Jet Propulsion Laboratory, Pasadena, Calif., Rept. TR 32-1329, Rev. 1, Jan. 15, 1970.

[4] Glaese, J.R., Kennel, H.F., Nurre, G.S., Seltzer, S.M., and Shelton, H.L., "Low Cost Space Telescope Pointing Control System," *Journal of Spacecraft and Rockets,* Vol. 13, July 1976, pp. 400-405.